

REPEATING THERMAL BRIDGES IN CEILINGS AND FLOORS: MODIFIED CALCULATION METHOD

STAGE 2 FINAL REPORT

9TH MARCH 2022

REVISED 29TH APRIL 2022

ABOUT THIS REPORT

Title: Repeating Thermal Bridges in Ceilings and Floors: Modified Calculation Method – Stage 2 Final Report

Authors: Alan Green, Steven Beltrame, Georgios Kokogiannakis and Paul Cooper

Acknowledgements: The authors would like to acknowledge the guidance and input provided by the Australian Building Codes Board. We would also like to thank members of the Thermal Bridging Subgroup of the Energy Efficiency Technical Working Group, who reviewed the modelling assumptions proposed for Stage 1 of this project and provided detailed feedback.

Contact details:

Sustainable Buildings Research Centre (SBRC)

Faculty of Engineering and Information Sciences

University of Wollongong

NSW 2522 Australia

Telephone: +61 (02) 4221 8111

Email: sbrc@uow.edu.au

Web: sbrc.uow.edu.au

Executive Summary

This report outlines the background, methodology and key findings from Stage 2 of an investigation into thermal bridging in ceiling and suspended floor assemblies. The study was commissioned by the Australian Building Codes Board (ABCB) and undertaken by the Sustainable Buildings Research Centre (SBRC) at the University of Wollongong.

During this second stage of the investigation, a new calculation method was developed to estimate the thermal resistance (R-value) of such building assemblies, which feature a thermally bridged construction layer exposed to an adjacent air space (i.e. the roof space or subfloor space). Previously existing calculation methods, including those in NZS 4214 [1] (which is specified under the NCC) and ISO 6946 [2], as well as the Modified Zone and Gorgolewski methods [3,4], do not account for several important features of ceilings and suspended floors, and therefore give rise to significant inaccuracies in many cases.

While we have developed empirical models for specific types of ceilings and floors in several previous studies [5–7], the focus in this report is on developing a method that is more generally applicable.

A set of 840 computational fluid dynamics (CFD) simulations were run to provide benchmark heat transfer performance data spanning a broad variety of construction details. Dimensionless parameter groups that efficiently correlate the data were identified, and an empirical function of the parameter groups was developed to calculate a correction factor, F , that can be used in NZS 4214 thermal bridge calculations. In addition to the use of this correction factor, the new calculation method also involves the inclusion of standard ‘film resistances’ on the thermally bridged layer where it is exposed to an air space. The film resistance can then be subtracted at the end of the calculation, to arrive at an R-value for the building assembly only, without a film resistance.

The accuracy of the new method was tested against the 840 CFD results from this study, as well as relevant CFD results from three previous studies also undertaken by the SBRC. Use of the new calculation method rather than the standard NZS 4214 method reduced the root mean square (RMS) deviation between calculated and simulated R-values:

- By 84 % (from 0.859 to 0.139 m² K W⁻¹) in the cases simulated in this study;

- By 89 % (from 0.690 to 0.078 m² K W⁻¹) in the cases simulated the original ABCB study [5];
- By 86 % (from 0.695 to 0.094 m² K W⁻¹) in the NASH study [6];
- By 40 % (from 0.435 to 0.259 m² K W⁻¹) in ceiling cases simulated in Stage 1 of this study [7]; and
- By 79 % (from 0.497 to 0.102 m² K W⁻¹) in floor cases simulated in Stage 1 of this study [7].

The largest improvements occurred in cases involving steel thermal bridges that are not mitigated by additional insulation or thermally broken by battens. Benefits of the new method were typically smaller when applied to other assemblies, but significant improvements were also found in cases involving timber-framed assemblies with insulation much taller than the thermal bridges, cases with thermal bridge mitigation, and cases with battens.

The primary value of the new calculation method lies in its general applicability, and its ability to avoid the most significant sources of inaccuracy that affect standard calculation methods. We recommend that the new method be used rather than the standard NZS 4214 method (or similar methods, such as the Modified Zone or Gorgelewski methods) when calculating the R-value of ceiling or floor assemblies in which the thermally bridged layer is exposed to the adjacent air space.

The new calculation method is an improved version of the one-dimensional method of NZS 4214, and models heat flows that are in reality complex and three-dimensional. As with all such simplified one-dimensional methods, the new method therefore cannot be expected to reliably provide results that are as accurate as data from experiments or detailed numerical simulations (e.g. CFD), and in some situations inaccuracies may still be significant. For example, in several outlying cases that were tested in the present project the new calculation method gave rise to inaccuracies in the order of 0.7 m² K W⁻¹, corresponding to approximately 20 % of the total assembly R-value. Nevertheless, in all such cases the new calculation method still reduced the inaccuracy of calculated R-values significantly, as compared to the standard NZS 4214 method.

In situations where the risk of such inaccuracy is not acceptable, we recommend that data from experiments or numerical simulations be used. One effective approach is to use the new calculation method proposed here, but with a correction factor F calibrated to benchmark

experimental or numerical simulation data for the specific, narrow set of building assemblies that are of interest. This approach has been taken in developing the tables of alternative thermal bridge mitigation measures presented in Section 4 of this report.

Table of contents

1	INTRODUCTION.....	1
1.1	Background.....	1
1.2	Project Aims.....	4
2	METHODOLOGY.....	6
2.1	Cases Simulated.....	7
2.1.1	Construction Details.....	7
2.1.2	Boundary Conditions.....	9
2.2	Calculation Method Development.....	11
2.2.1	Treatment of Film Resistances.....	13
2.3	Validation.....	13
3	MODEL DESCRIPTION AND PERFORMANCE.....	14
3.1	Description of New Calculation Method.....	14
3.2	Example Implementation.....	16
3.2.1	Suspended Floor.....	16
3.2.2	Ceiling with Battens.....	18
3.3	Performance of the New Method.....	20
3.3.1	Performance within the Present Dataset.....	20
3.3.2	Validation Against Previous Results.....	23
4	ALTERNATIVE DTS MITIGATION MEASURES.....	26
5	CONCLUSION.....	29
	REFERENCES.....	30
	APPENDICES.....	31
	Appendix A: CFD Methodology.....	31

List of abbreviations

ABCB	Australian Building Codes Board
ASHRAE	American Society of Heating, Refrigerating and Air-Conditioning Engineers
CFD	Computational fluid dynamics
DTS	Deemed to satisfy
NASH	National Association of Steel-Framed Housing
NCC	National Construction Code
RMS	Root mean square
R-value	Effective thermal resistance [$\text{m}^2 \text{K W}^{-1}$]
SBRC	Sustainable Buildings Research Centre

1 Introduction

This is the final report on Stage 2 of an investigation into thermal bridging in ceiling and suspended floor assemblies caused by ‘repeating’ frame members (i.e. regularly spaced thermal bridges, such as roof trusses or floor joists). The project was undertaken by the Sustainable Buildings Research Centre (SBRC) at the University of Wollongong, for the Australian Building Codes Board (ABCB).

1.1 BACKGROUND

The research presented in this report builds on the findings of several recent projects completed by the SBRC on the same topic, including the following.

- An initial investigation into the accuracy of standard thermal resistance (R-value) calculation methods when applied to thermally bridged ceiling assemblies [5]. Existing methods were found to overestimate the severity of metal thermal bridges when the roof space above ceilings is not included in the calculations, typically producing R-value estimates 15–64 % lower than reference values determined through computational fluid dynamics (CFD) simulations. A modified calculation method was proposed, which followed the standard NZS 4214 ‘isothermal planes’ methodology but with the addition of a ‘pseudo air-space’ R-value ($R_{pa} = 0.3 \text{ m}^2 \text{ K W}^{-1}$). Once the calculation is complete, R_{pa} is subtracted from the result to arrive at an R-value for the ceiling assembly alone. Due to the relatively small set of ceiling constructions simulated in that study, it was recommended that further investigations be carried out to test the modified calculation method over a broader range of scenarios and make further adjustments to the method if needed.
- An extension on the original project was subsequently undertaken for the National Association of Steel-Framed Housing (NASH). The investigation focused on ceilings with: i) ceiling battens installed between the frame and plasterboard ceiling lining, ii) partial or complete ‘encapsulation’ of frame members by the adjacent insulation, and iii) a thinner (0.75 mm) steel frame member base metal thickness, amongst other changes [6]. CFD simulations were used to determine the R-values of such ceilings, and physical tests were undertaken to demonstrate the degree of frame ‘encapsulation’ that occurs given a variety of insulation R-values, frame spacings, frame materials, and insulation materials. Results from this study

complemented findings from the previous investigation [5], by providing insights into aspects of ceiling thermal bridging that were not covered previously.

- Stage 1 of the current project [7] extended the investigations undertaken in the previous two studies described above. CFD simulations were used to quantify thermal bridging effects in:
 - Horizontal ceilings under pitched roofs, with timber or steel frames, a variety of insulation R-values, ceiling battens installed under the frame, 0.75 mm steel frame base metal thickness, timber thermal conductivity of $0.12 \text{ W m}^{-1} \text{ K}^{-1}$, and with or without thermal bridge mitigation measures prescribed in the draft NCC 2022 Housing Provisions; and
 - Suspended floor assemblies with timber or steel frames, a variety of insulation R-values, and with or without thermal bridge mitigation measures prescribed in the draft NCC 2022 Housing Provisions.

A set of separate models were developed for each of these types of assemblies, incorporating empirically determined pseudo air-space R-values (R_{pa}). Analyses were also undertaken to demonstrate sources of inaccuracy in the standard R-value calculation methods when applied to flat, skillion and cathedral roofs, and it was recommended that the treatment of ventilated air spaces in AS/NZS 4859.2 be reviewed.

A literature review developed in the first of the studies described above [5] provides an overview of R-value calculation methods that have been developed previously and are in current use under building regulations in various jurisdictions. Essentially, all existing methods are based on some combination of two fundamental approaches: the isothermal planes and the parallel path methods. For example, ISO 6946 [2] instructs users to take the average of the isothermal planes and parallel path calculation results, and methods such as the Modified Zone method [3,8] and the Gorgolewski method [4,9] use coefficients calibrated against finite element thermal simulations to produce a weighted average.

The Australian National Construction Code (NCC) currently specifies that methods outlined in AS/NZS 4859.2 be used to determine the R-value of building assemblies, which, in turn, requires methods in NZS 4214 to be followed for thermal bridge calculations. NZS 4214 prescribes a version of the isothermal planes method developed by Trethowen *et al.* at the Building Research Association of New Zealand (BRANZ) [10].

Each of these existing calculation methods has been validated for use on certain types of building assemblies. For example the NZS 4214 method has been shown to estimate thermal bridging effects accurately for 84 typical timber-framed and steel-framed wall and roof assemblies [10]. However, the accuracy of such calculations when applied to ceiling and suspended floor assemblies does not appear to have been studied in detail prior to our original project for the ABCB [5].

When existing thermal bridge calculation methods are used to estimate the R-value of some ceilings and suspended floors significant inaccuracies (in the order of 50 % in some cases) can arise. These are caused by contributions from several limitations in the existing methods, as outlined below and illustrated in Figure 1.

1. When applied to ceiling or floor assemblies in isolation, without including the adjacent air space (i.e. roof space or subfloor space) in the calculation, the temperatures of the surfaces exposed to those air spaces are inherently assumed to be isothermal. For example, the top surface of ceiling joists and insulation exposed to a roof space are assumed to be at the same uniform temperature. This assumption can be highly unrealistic, especially in cases with severe thermal bridges, and gives rise to significant inaccuracy in the calculated R-value.
2. When the height of such thermal bridges is different to that of the surrounding bulk insulation, the exposure of the thermal bridges to convective and radiant heat transfer within the air space can be enhanced (if the thermal bridges protrude beyond the insulation) or mitigated (if the bridges are recessed beneath the surface of the insulation), and existing calculation methods do not account for these effects.
3. The partial ‘shielding’ of exposed thermal bridges from radiant and convective heat transfer can be further increased if bulk insulation partially or fully ‘encapsulates’ the thermal bridges.
4. When the thermal emittance, ε , of the exposed surfaces of thermal bridges differs from that of the surrounding insulation, e.g. when bare metal frame members ($\varepsilon \approx 0.25$) are exposed between ceiling batts ($\varepsilon \approx 0.9$), then radiant heat transfer to/from the thermal bridges can be significantly different to that assumed in standard calculations.
5. Additional inaccuracies can arise due to the simplistic representation of complex three-dimensional heat transfer processes by a one-dimensional thermal network. Existing thermal bridge calculation methods, such as the Modified Zone and Gorgolewski methods, have been developed to minimise this type of inaccuracy when applied to certain types of building

assemblies. However, significant inaccuracies can still arise if the methods are applied outside of the range of cases on which the model coefficients were established.

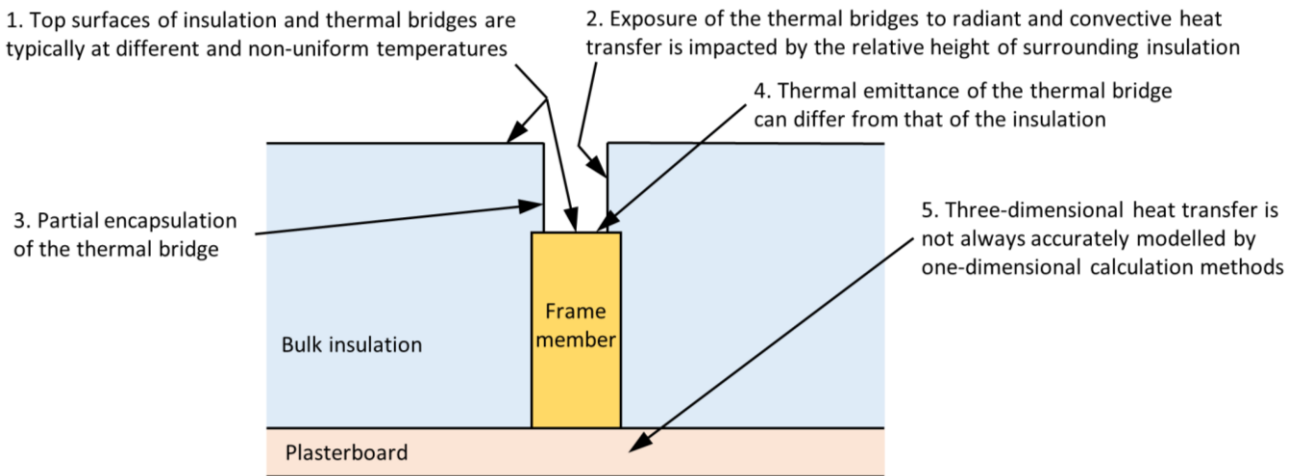


Figure 1: Factors that can contribute to the inaccuracy of the standard NZS 4214 calculation method when applied to ceilings and suspended floors. Numbers correspond to the sources of inaccuracy listed in the text above the figure.

The first four sources of inaccuracy listed above do not arise in building assemblies where the thermally bridged layer is ‘sandwiched’ between homogeneous material layers, such as in typical Australian wall construction. Several existing thermal bridge calculation methods, including the NZS 4214, Modified Zone and Gorgolewski methods, have been shown to produce accurate results when applied to such building assemblies. However, building assemblies that include an exposed thermally bridged layer on one surface, such as typical Australian ceilings and suspended floors, can give rise to any of the five sources of inaccuracy listed above. It appears to be this characteristic of such assemblies that causes previously established calculation methods to become as inaccurate as they have been shown to be in our recent investigations.

1.2 PROJECT AIMS

In Stage 2 of the current project, the SBRC was commissioned by the ABCB to develop a method to calculate the R-value of thermally bridged horizontal ceilings under pitched roofs that is more accurate than existing methods. While improved calculation methods have been proposed in our previous reports [5,7], they relied on coefficients that were fitted to CFD data from relatively narrow sets of cases; the new method developed as a result of the work described here was required to be more broadly applicable.

Due to the similarities between ceiling assemblies and suspended floor assemblies, and the common issues that arise when existing calculation methods are applied to them, the new calculation method was also developed for application to suspended floors.

This report outlines the methodology and key results of the study.

2 Methodology

To produce a new calculation method that could correct for the various sources of inaccuracy outlined in Section 1.1, a reference dataset needed to be generated that covered such a wide range of scenarios (e.g. different ceiling or floor construction details). By producing a dataset that covered a wider range of construction details, it was also possible to disaggregate the effects of each source of inaccuracy, to an extent. For example, the influence of the emittance of exposed surfaces of thermal bridges could be quantified in isolation from other sources of inaccuracy, before the combined influence of multiple sources of inaccuracy was investigated.

As in our previous studies, computational fluid dynamics (CFD) was used to produce the required reference data. Two-dimensional and three-dimensional steady-state conjugate heat transfer CFD simulations were run to quantify the R-value of thermally bridged horizontal ceilings with top surfaces exposed to an adjacent roof space. While the assemblies were modelled as ceilings (with an airspace above), the findings are also relevant to suspended floors (with air spaces below). More detail on the CFD methods and settings is provided in Appendix A, and details of the cases simulated, boundary conditions, etc. are provided in Section 2.1 below.

To allow the large number of ceiling/floor assemblies to be simulated in a manageable timeframe, thermal bridges were modelled as solid rectangular prisms in all simulations. Thus, steel frame members (e.g. joists, truss chords and battens) were modelled as ‘equivalent’ solid rectangles, in the same way that they are represented within the NZS 4214 calculation method. The thermal conductivity of the ‘equivalent’ solid rectangles was calculated assuming a thermal conductivity of $47.5 \text{ W m}^{-1} \text{ K}^{-1}$ for steel. Several CFD simulations run with this approach were compared to otherwise identical simulations performed in Stage 1 [7], in which steel frame geometries were modelled explicitly, and the resulting R-values were found to be within 1 % of the Stage 1 results.

Results from the CFD simulations were analysed and used as the basis for the new calculation method, as described in Section 2.2, and the calculation method was also validated against CFD results from our previous studies.

2.1 CASES SIMULATED

2.1.1 Construction Details

A total of 840 CFD simulations were performed, to investigate various combinations of the ceiling/floor assembly parameters outlined in Table 1. The range of values assigned to each parameter was selected to approximately represent the range of typical ceiling and suspended floor assemblies in Australian buildings.

Table 1: Parameters investigated in the parametric CFD study.

Parameter	List of Values
Frame height [mm]	90, 140
Frame width [mm]	35, 40, 50
Frame encapsulation [mm]	0, 7.5, 10, 22.5
Frame effective thermal conductivity [$\text{W m}^{-1} \text{K}^{-1}$]	0.12, 1.018 ¹ , 2.036 ¹ , 0.8906 ¹ , 0.7125 ¹ , 1.425 ¹
Frame thermal emittance	0.05, 0.12, 0.25, 0.9
Frame centre-to-centre spacing [mm]	450, 600, 900
Insulation batt height [mm]	60, 75, 90, 110, 125, 140, 170, 200, 300
Insulation batt thermal conductivity [$\text{W m}^{-1} \text{K}^{-1}$]	0.025, 0.0375, 0.05
Internal lining thickness [mm]	10, 35
Internal lining R-value [$\text{m}^2 \text{K W}^{-1}$]	0.0589, 0.4589, 1.0589
Battens	Absent, Present
Batten height [mm]	20
Batten width ² [mm]	30
Batten effective thermal conductivity [$\text{W m}^{-1} \text{K}^{-1}$]	1.33 ³ , 2.375 ³
Batten centre-to-centre spacing [mm]	600
Thermal bridge mitigation	None, continuous insulation over frame, strips of insulation on top of frame members (see Figure 4)
Mitigation layer thickness [mm]	5, 9.75, 13, 19, 19.75, 20, 25.5,
Mitigation layer R-value [$\text{m}^2 \text{K W}^{-1}$]	0.0975, 0.1, 0.19125, 0.2, 0.26, 0.38, 0.51, 0.72

¹ Steel frame members were modelled as 'equivalent' solid rectangles, with thermal conductivity values calculated according to NZS 4214 and with an assumed base metal thickness of either 0.75 mm or 1.5 mm.

² The width of the equivalent rectangle used to represent ceiling battens (i.e. metal battens with an overall width of 60 mm and a flange contact width of 30 mm).

³ Steel battens were modelled as 'equivalent' solid rectangles, with thermal conductivity calculated according to NZS 4214 and with assumed base metal thickness of either 0.42 mm or 0.75 mm.

Cases without battens were simulated in two dimensions (Figure 2) whereas simulations with battens needed to be simulated in three dimensions (Figure 3) so that three-dimensional heat flow near the intersection of the frame members and the ceiling battens could be resolved. In cases with battens, only half the batten was modelled and a 'symmetry' boundary condition was used to model the influence of the other half of the batten, i.e. the computational domain included the section of assembly from the vertical mid-plane of one batten to the vertical plane half-way between it and the adjacent batten.

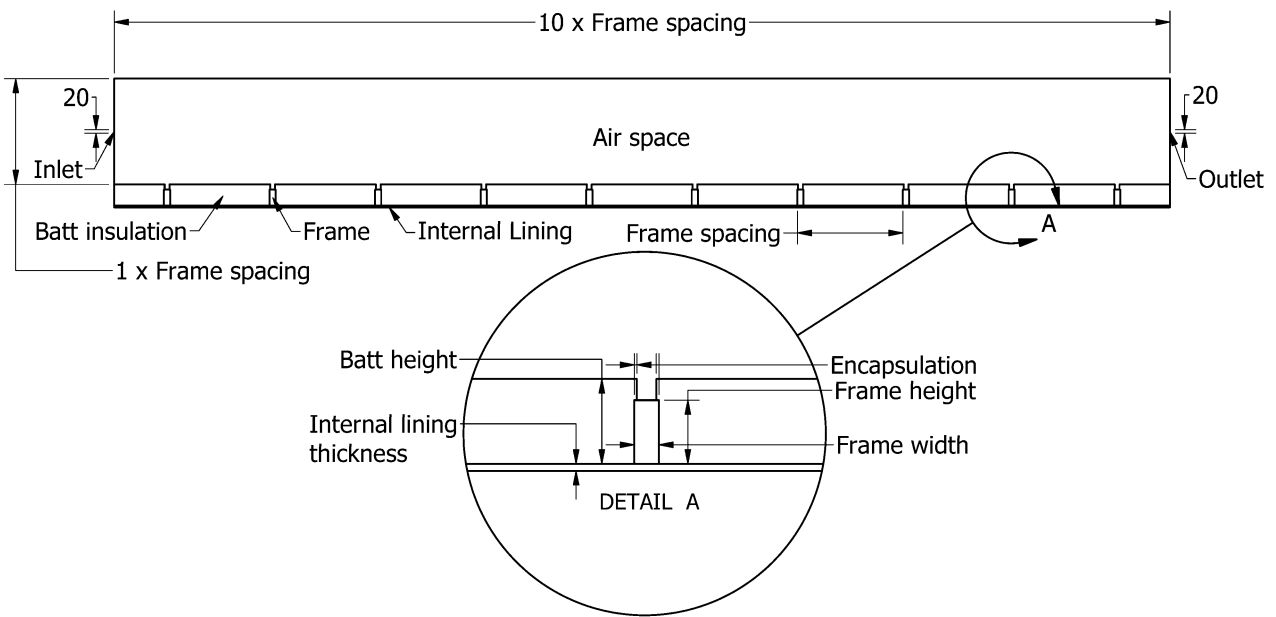


Figure 2: Example of the two-dimensional computational domain developed for the CFD simulations of horizontal assemblies with top surfaces exposed to an air space.

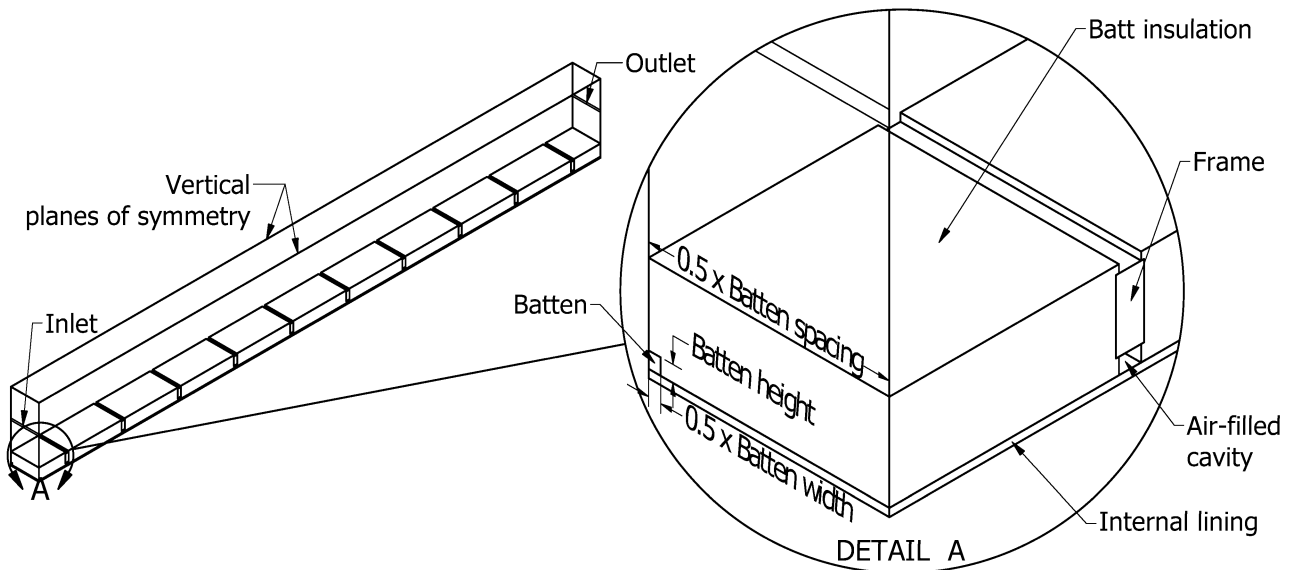


Figure 3: Example of the three-dimensional computational domain developed for CFD simulations of horizontal assemblies with battens. Note that a symmetry boundary condition was applied at the vertical plane that bisects the batten.

The computational domain defined for each simulation contained ten frame members, and the height of the rectangular adjacent air space (representing the roof space) was set equal to 10 % of its width. The inlet and outlet to the air space were defined as 20 mm-high slot openings at opposite ends of the air space.

In cases with thermal bridge mitigation measures, the geometry of the fit of the additional insulation around other components in the assembly depended on the type of mitigation and the relative heights of the batts and the frames, as shown in Figure 4.

Contact resistances of $0.03 \text{ m}^2 \text{ K W}^{-1}$ were included at the interfaces between any two rigid materials in contact (i.e. between timber or steel frame members and battens, between frame members and lining, and between battens and lining).

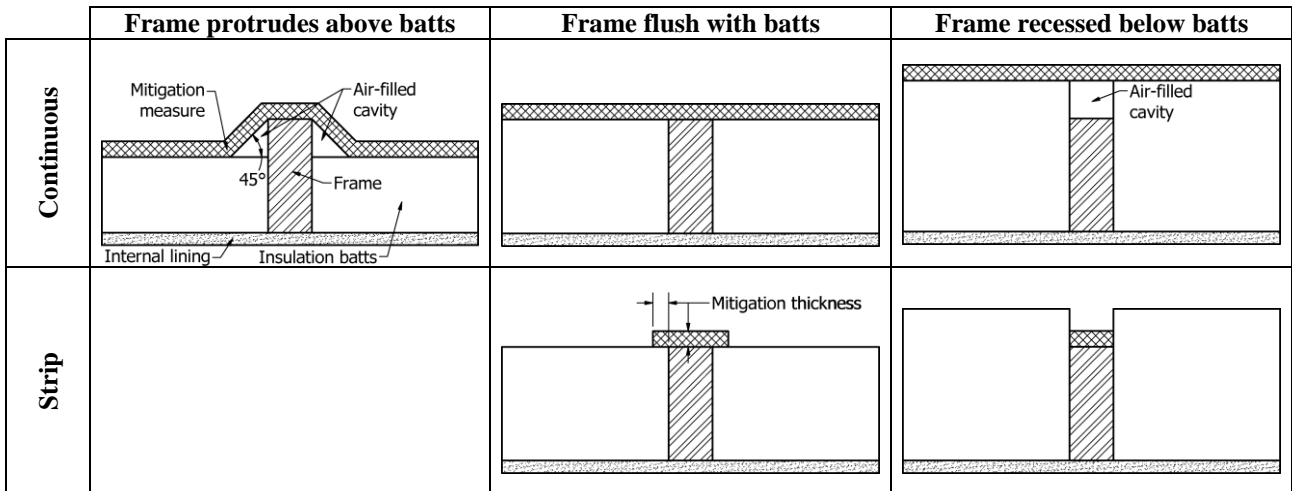


Figure 4: Examples that demonstrate how strip and continuous mitigation measures were applied for different combinations of batt and frame heights. Note that strip mitigation measures were not examined in cases where the frame protruded above the batts. These partial cross-sections are used to highlight the mitigation geometry and do not illustrate the full computational domain modelled in cases with mitigation measures, which were similar to those shown in Figure 2 and Figure 3.

2.1.2 Boundary Conditions

In previous studies [5], we found that the R-values of ceiling assemblies (not including ‘film resistances’) determined from CFD simulations were not significantly influenced by changes in boundary conditions (e.g. different roof space ventilation rates, outdoor air temperature, etc.), within the range of boundary conditions relevant to roofs. However, this does not mean that the R-value of the building envelope as a whole is unaffected by boundary conditions; the R-value of roof spaces can change significantly under different operating conditions. Therefore, one primary set of boundary conditions was defined and applied to the majority of simulations, and a relatively small set of additional simulations were run with alternative boundary conditions to determine the sensitivity of results to those settings.

The ‘primary settings’ of the boundary conditions applied in this study and the ‘additional cases tested’ are outlined in Table 2. These boundary conditions were based on simulations [5] of entire

roof/ceiling assemblies operating under summer daytime conditions. Since the fundamental convection and conduction processes for ceiling assemblies and suspended floor assemblies are inverted but otherwise identical, the boundary conditions used in this study are equally applicable to both situations. It was important only that the ‘primary settings’ of the boundary conditions were of the same order of magnitude as those typically encountered in roof and subfloor spaces in real buildings, and that the ‘additional cases tested’ represented more extreme values of boundary conditions within the range expected to occur in reality. By following this approach, the simulations provided sufficient information on the fundamental nature of heat transfer within ceiling and floor assemblies to facilitate the development of the new method.

Table 2: Boundary conditions applied in the parametric CFD study.

Parameter	Primary setting	Additional cases tested
Indoor temperature	22 °C	-
Indoor ‘film resistance’	0.16 m ² K W ⁻¹	<ul style="list-style-type: none"> • 0.16 m² K W⁻¹ (downward heat flow) • 0.11 m² K W⁻¹ (upward heat flow)
Air space air inlet temperature	35 °C	<ul style="list-style-type: none"> • 5 °C
Air space air change rate	10 h ⁻¹	<ul style="list-style-type: none"> • 5 h⁻¹ • 20 h⁻¹
Temperatures of surfaces bounding the top and sides of the air space	35 °C	<ul style="list-style-type: none"> • 5 °C • 22 °C • 50 °C
Thermal emittance of surfaces bounding the top and sides of the air space	0.9	-

2.2 CALCULATION METHOD DEVELOPMENT

To overcome the limitations of existing thermal bridge calculation methods, as described in Section 1.1, the simulation outputs were used to develop a calculation method.

The new calculation method was developed with the following general form:

$$R = \sum_i R_{h_i} + R_b = \sum_i R_{h_i} + \left(\frac{1}{F} \sum_j \frac{f_{tb_j}}{R_{tb_j}} + \sum_k \frac{f_{in_k}}{R_{in_k}} \right)^{-1} \quad (1)$$

where:

R is the R-value of the assembly;

R_{h_i} is the R-value of the i th continuous homogeneous layer, i.e. a layer outside the ‘bridged layer(s)’;

R_b is the thermal resistance through the bridged portion of the assembly;

f_{tb_j} is the area fraction of the j th heat flow path through the frame member within the thermally bridged layer(s);

f_{in_k} is the area fraction of the k th heat flow path through the insulating material of the thermally bridged layer(s);

R_{tb_j} is the total R-value of the j th heat flow path through the frame member within the thermally bridged layer(s), and should include ‘film resistances’ if those components are exposed to an adjacent air space;

R_{in_k} is the total R-value of the k th heat flow path through the insulating material of the thermally bridged layer(s), and should include ‘film resistances’ if those components are exposed to an adjacent air space; and

F is a correction factor made to the heat flow paths through the frame member.

This method is identical to the standard NZS 4214 method, except for two adjustments:

1. Standard ‘film resistances’ are included in the calculation where a thermally bridged layer is adjacent to an air space, and the same film resistances can be subtracted from R to arrive at an R-value for the building assembly alone (refer to Section 2.2.1).
2. The correction factor F is used to counteract inaccuracies introduced by the issues outlined in Section 1.1.

This approach is different to the calculation methods proposed in our previous reports [5–7], where a ‘pseudo air-space R-value’ was included instead of standard film coefficients and F . The benefit of the new approach proposed here is that, where the previously proposed methods could become numerically unstable when the denominators in fractions approached zero, the denominators in Equation 1 cannot equal zero while F is non-zero so the calculation method avoids such numerical instability.

An equation for the correction factor F was developed using data from the parametric CFD study, as outlined in the list of primary steps below.

1. Identify dimensionless parameter groups that capture important aspects of independent parameters within the dataset (e.g. dimensional and thermal characteristics of components such as frames and insulation batts, surface emittances, etc.).
2. Test for correlations between the parameter groups and the correction factor, F .
3. Iterate through steps 1 and 2 until parameter groups have been discovered that collapse the dataset as far as possible into a single trend.
4. Describe F as a function of the final set of dimensionless parameter groups.

When applying the NZS 4214 calculation method, or our modified version of that method, the following approach was taken.

- The guidelines developed by Trethowen [10] were followed where relevant.
- When applied to assemblies with battens, four heat transfer pathways were identified through:
 - i. The batt insulation;
 - ii. The frame and cavity formed between the frame and internal lining;
 - iii. The battens and batts; and
 - iv. The battens and frame.
- The effective R-values of any cavities formed within the assembly (e.g. between frame members and the internal lining) were determined using methods specified in Appendix D of ISO 6946 [2].
- Thermal contact resistances of $0.03 \text{ m}^2 \text{ K W}^{-1}$ were included between any two rigid components (e.g. battens, timber or steel frame members, and lining materials) in contact with each other.

2.2.1 Treatment of Film Resistances

There are two types of ‘film resistances’ relevant to this calculation method:

- a) the ‘film resistance’ at the exposed surface of a building assembly where a *continuous homogeneous layer* is exposed to an adjacent air space; and
- b) the ‘film resistance’ at the exposed surface of a building assembly where a *thermally bridged layer* is exposed to an adjacent air space.

The first type of ‘film resistance’ can be included within the sum of the thermal resistances of continuous homogeneous layers, i.e. $\sum_i R_{h_i}$ within Equation 1. This ‘film resistance’ does not need to be included in the calculation when a user is interested in calculating the R-value of the assembly alone (i.e. a ‘surface to surface’ R-value). In this study we have not included this ‘film resistance’ as we wished to calculate ‘surface to surface’ R-values in order to be consistent with previous reports and the NCC provisions, and to be compatible with precursor NatHERS simulations.

As explained in Section 2.2, the second type of ‘film resistance’ *must* be included separately within each heat flow path when applying the new calculation method (i.e. within the R_{tb_j} and R_{in_k} terms in Equation 1) for all cases involving a thermally bridged layer exposed to an adjacent air space. Inclusion of this ‘film resistance’ in each path is necessary to numerically address ‘Issue 1’ listed in Section 1.1. This ‘film resistance’ can be subtracted at the end of the calculation to calculate the ‘surface to surface’ R-value, as was done in this report, and demonstrated in the worked examples in Section 3.2. (Note that the inclusion of ‘film resistances’ within the calculation means that the resulting R-values will be somewhat dependent on the direction of heat flow relative to gravity, even if the ‘film resistances’ are subtracted at the end of the calculation.)

2.3 VALIDATION

The new calculation method developed in this study was validated against R-values determined from CFD simulations in our two previous studies [5,6], and in Stage 1 of the present study [7], where the steel frame geometries were fully meshed/resolved. At the time of writing we are not aware of other data in the public domain that are suitable for validation of the new calculation method.

3 Model Description and Performance

3.1 DESCRIPTION OF NEW CALCULATION METHOD

Analysis of the CFD data revealed that a relatively close agreement could be achieved between calculated and simulated R-values using the following equation for the correction factor F defined in Equation 1.

$$F = C_1 + C_2 \left(\frac{R_u w_b}{R_b h_b} \right) + C_3 \left(\frac{0.9 - \varepsilon_b}{0.9} \right) + C_4 \ln \left(\frac{h_b + h_B}{h_u + h_U} \right) + C_5 \left(\frac{w_b - x}{w_b} \right) \quad (2)$$

Where each parameter is defined as follows.

\ln is the natural logarithm.

R_u is the R-value of the heat flow path through the insulating material within the thermally bridged layer. (For cases with more than one heat flow path through the insulating material, R_u is taken as the R-value of the path with the largest area fraction).

R_b is the R-value of the heat flow path through the frame member within the thermally bridged layer. (For cases with more than one heat flow path through the frame member, R_b is taken as the R-value of the path with the largest area fraction).

w_b is the width of the thermal bridges (e.g. frame members).

h_b is the height of the thermal bridges.

h_B is the height of any cavities, battens or other components that contribute to the total height of materials in the heat flow path through the frame member within the thermally bridged layer.

h_u is the height of the insulating material surrounding the thermal bridges.

h_U is the height of any cavities, battens or other components that contribute to the total height of materials in the heat flow path through the insulating material within the thermally bridged layer.

ε_b is the thermal emittance of the exposed surface of the thermal bridges.

x is the width of the gap formed above each thermal bridge (if there is no encapsulation $x = w_b$, if the surrounding batts do encapsulate frame members $x < w_b$).

C_1, C_2, C_3, C_4 and C_5 are model coefficients.

Figure 5 is a schematic representation of the key parameters mentioned above.

Within the broad set of non-dimensional parameter groups that were tested, those included in Equation 2 produced the best overall ‘performance’ of the model, i.e. in terms of the least squares fit of the model to the data.

The first two terms in Equation 2 effectively account for inaccuracies in the NZS 4214 calculation method in relatively simple cases where the thermal bridge and surrounding material have equal heights and emittance (in such cases, the other three terms go to zero). The third and fourth terms in the equation account for the influence of differences in emittance or height, respectively, between the bridges and surrounding materials, and the fifth term accounts for the effects of encapsulation.

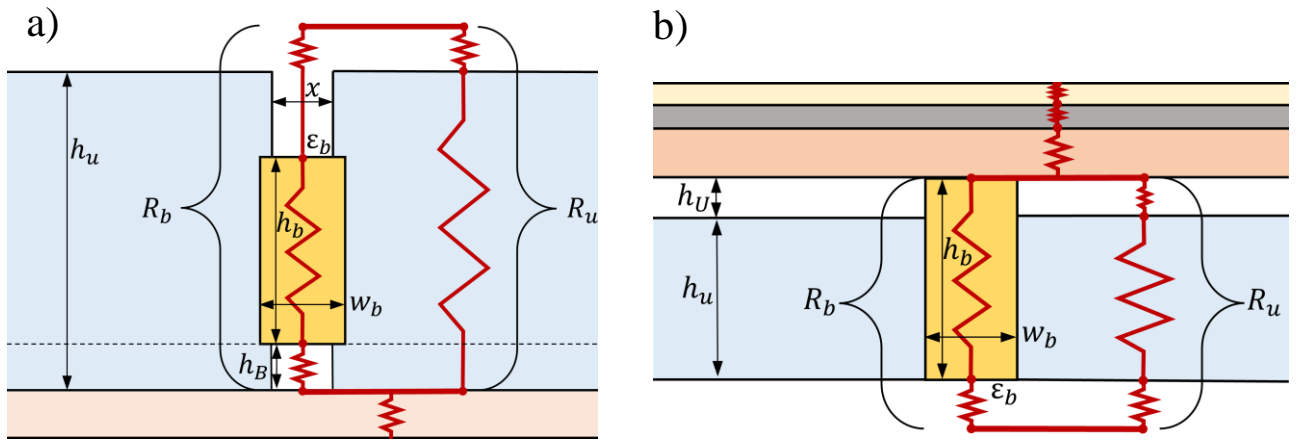


Figure 5: Partial cross-section of a thermally bridged (a) ceiling with battens oriented perpendicular to the joist, and (b) suspended floor, showing key parameters used in Equation 2.

The numerical values of the coefficients in Equation 2 were established by a least-squares optimisation using the CFD data, and are presented in Table 3. Three sets of coefficients are presented: the first set forms a model that can be applied to both timber-framed or steel-framed assemblies, and the second and third sets of coefficients provide slightly better performance when applied specifically to either timber-framed or steel-framed assemblies, respectively, as indicated in Table 3.

We recommend that the separate ‘timber only’ and ‘steel only’ models be used when it is practicable to do so, but the combined ‘timber or steel’ model could be more convenient in some situations.

Table 3: Coefficients developed for use in Equation 2.

Model	Model coefficients				
	C_1	C_2	C_3	C_4	C_5
Timber or steel	0.72	0.079	0.34	0.072	0.67
Timber only	0.91	0.06	0.14	0.26	0.38
Steel only	0.72	0.058	0.46	-0.29	0.87

Within the set of cases simulated in this stage of the project, the root mean square (RMS) deviation between R-values determined through CFD and calculations was $0.859 \text{ m}^2 \text{ K W}^{-1}$ when the standard NZS 4214 calculation method is used, which was reduced (by 80 %) to $0.168 \text{ m}^2 \text{ K W}^{-1}$ when the combined ‘timber or steel’ model was used, and (by 84 %) to $0.139 \text{ m}^2 \text{ K W}^{-1}$ when the separate ‘timber only’ and ‘steel only’ models were used. Further information on the model performance is provided in Section 3.3.

Equations 1 and 2, and the coefficients in Table 3 comprise the new calculation method. Note that, as it is a modified version of the standard NZS 4214 method, the instructions contained in that standard are also needed to fully describe the new method, and (as highlighted in our previous report) additional guidance based on the work of Trethowen [10] should be provided to users to assist them in defining bridged layers and heat flow paths appropriately. A worked example is provided below.

3.2 EXAMPLE IMPLEMENTATION

Two worked examples are provided below, demonstrating the application of the new calculation method to a suspended floor and a ceiling assembly with battens.

3.2.1 Suspended Floor

If the new calculation method was applied to a suspended floor with 100 mm (high) \times 50 mm (wide) \times 1.5 mm (base metal thickness) steel frame members installed with a frame factor of 10.8 % and R2, 75 mm-tall batt insulation installed ‘low’ (i.e. flush with the lower flange of the frame members) under: (i) 22 mm-thick particleboard (R0.2037), (ii) 10 mm-thick underlay (R0.0198), and (iii) 10 mm-thick carpet (R0.1379), the following procedure would be followed. The thermal conductivity of steel is set equal to $47.5 \text{ W m}^{-1} \text{ K}^{-1}$, and the emittance of the steel frame is assumed to be 0.28 for upward-facing surfaces and 0.23 for downward-facing surfaces. This assembly is similar to that shown in Figure 5 b).

Following procedures outlined in NZS 4214, the thermal resistance of an ‘equivalent’ solid rectangle representing the frame members is given by $R_f = 0.1 \times 0.05 / (47.5 \times 0.0015) = 0.070175 \text{ m}^2 \text{ K W}^{-1}$.

The thermally bridged layer includes the batts and frame members, but not the homogeneous layers above, so the total R-value of unbridged layers (i.e. particleboard, underlay and carpet) is given by $\sum_i R_{hi} = R_{p_1} + R_{p_2} + R_{p_3} = 0.2037 + 0.0198 + 0.1379 = 0.3614 \text{ m}^2 \text{ K W}^{-1}$. Within the thermally bridged layer, two separate heat transfer paths can be defined, as follows.

- A. A path through the frame members, with area fraction equal to the frame factor $f_A = 0.108$, and an R-value of $R_A = R_{film} + R_f + R_c = 0.260175 \text{ m}^2 \text{ K W}^{-1}$, where $R_{film} = 0.16 \text{ m}^2 \text{ K W}^{-1}$ is the film resistance for downward heat flow from AS/NZS 4859.2 (applied here to the exposed bottom surface of the frame member) and $R_c = 0.03 \text{ m}^2 \text{ K W}^{-1}$ is the standard contact resistance from NZS 4214.
- B. A path through the batts, with area fraction $f_B = (1-0.108) = 0.892$, and an R-value of $R_B = R_{film} + 2 + R_{cav} = 2.3275 \text{ m}^2 \text{ K W}^{-1}$, where $R_{cav} = 0.1675 \text{ m}^2 \text{ K W}^{-1}$ is the R-value of the 25 mm cavity formed between the batts and particleboard above, calculated according to Appendix D of ISO 6946.

Note that in this new calculation method, the film resistance R_{film} is included in each heat transfer pathway since each is exposed to the adjacent subfloor space.

The correction factor F can then be calculated using Equation 2 and using the ‘steel only’ coefficients from Table 3, as follows.

$$F = 0.72 + 0.058 \left(\frac{2.3275 \times 0.05}{0.260175 \times 0.1} \right) + 0.46 \left(\frac{0.9 - 0.23}{0.9} \right) - 0.29 \ln \left(\frac{0.1 + 0}{0.075 + 0.025} \right) + 0.87 \left(\frac{0.05 - 0.05}{0.05} \right)$$

$$F = 1.321876$$

Insertion of this correction factor into the modified NZS 4214 equation for the ceiling R-value (Equation 1), yields:

$$R = \sum_i R_{n_i} + \left(\frac{1}{F} \sum_j \frac{f_{tbj}}{R_{tbj}} + \sum_k \frac{f_{in_k}}{R_{in_k}} \right)^{-1} - R_{film}$$

$$R = R_{p_1} + R_{p_2} + R_{p_3} + \left(\frac{1}{F} \left(\frac{f_A}{R_A} \right) + \frac{f_B}{R_B} \right)^{-1} - R_{film}$$

$$R = 1.636 \text{ m}^2 \text{ K W}^{-1}$$

Note that the correction factor F is only applied to paths that contain the thermal bridge, and that the film resistance R_{film} is subtracted from the total R-value to arrive at a result that does not include film resistances (i.e. a ‘surface to surface’ R-value).

This result can be compared to an identical case in Stage 1 of this project, for which CFD simulation predicted an R-value of 1.7002 m² K W⁻¹, differing from the value calculated here by approximately 4 %.

3.2.2 Ceiling with Battens

If the new calculation method was applied to a ceiling with 90 mm (high) × 40 mm (wide) × 0.75 mm (base metal thickness) steel frame members installed with a frame factor¹ of 6 % over a 10 mm-thick plasterboard lining fitted to 20 mm (high) × 30 mm (flange width) × 0.42 mm (base metal thickness) steel battens installed at 600 mm centres, with R3, 144 mm-tall ceiling batts and zero encapsulation, the following procedure would be followed. The thermal conductivity of steel and plasterboard are set equal to 47.5 and 0.17 W m⁻¹ K⁻¹, respectively, and the emittance of the steel frame is assumed to be 0.28 for upward-facing surfaces and 0.23 for downward-facing surfaces. It is assumed that the upper surface of the ceiling batts is flat, i.e. the batts are partially compressed above the battens.

Following procedures outlined in NZS 4214, the thermal resistance of an ‘equivalent’ solid rectangle representing the frame members is given by $R_f = 0.09 \times 0.04 / (47.5 \times 0.00075) = 0.1011 \text{ m}^2 \text{ K W}^{-1}$. Likewise, the steel battens can be modelled as equivalent solid rectangles with $R_b = 0.02 \times 0.03 / (47.5 \times 2 \times 0.00042) = 0.0150 \text{ m}^2 \text{ K W}^{-1}$.

The thermally bridged layer includes the batts, frame members and battens. The plasterboard is the only continuous homogeneous layer (i.e. layer outside of the ‘bridged layer’) within the assembly. The total R-value of the continuous homogeneous layers is therefore the thermal resistance of the plasterboard layer, which is given by $\sum_i R_{h_i} = R_p = 0.01 / 0.17 = 0.0588 \text{ m}^2 \text{ K W}^{-1}$. Within the thermally bridged layer, four separate heat transfer paths can be defined, as follows.

- A. A path through the frame members where they are directly above battens, with area fraction $f_A = 0.06 \times 0.03 / 0.6 = 0.003$, and an R-value of $R_A = R_{film} + R_f + R_c + R_b + R_c = 0.3361 \text{ m}^2 \text{ K W}^{-1}$, where $R_{film} = 0.16 \text{ m}^2 \text{ K W}^{-1}$ is the film resistance for downward heat flow from AS/NZS 4859.2 (applied here to the exposed top surface of the frame member) and $R_c = 0.03 \text{ m}^2 \text{ K W}^{-1}$ is the standard contact resistance from NZS 4214.

¹ Frame factor equals the fraction of the projected area of the assembly that is occupied by frame members.

- B. A path through the frame members where they are not above a batten, with area fraction $f_B = 0.06 \times (1 - 0.03/0.6) = 0.057$, and an R-value of $R_B = R_{film} + R_f + R_{cav} = 0.6493 \text{ m}^2 \text{ K W}^{-1}$, where $R_{cav} = 0.3882 \text{ m}^2 \text{ K W}^{-1}$ is the R-value of the 20 mm cavity formed between the frame members and plasterboard below, calculated according to Appendix D of ISO 6946.
- C. A path through the batts and the battens, with area fraction $f_C = (1 - 0.06) \times 0.03/0.6 = 0.047$, and an R-value of $R_C = R_{film} + R_{comp} + R_b + R_c = 2.9967 \text{ m}^2 \text{ K W}^{-1}$, where $R_{comp} = 2.7917 \text{ m}^2 \text{ K W}^{-1}$ is R-value of the batt insulation where it is compressed above each batten, according to the rule of thumb in Appendix C of NZS 4214.
- D. A path through the batts where they are not above a batten, with area fraction $f_D = (1 - 0.06) \times (1 - 0.03/0.6) = 0.893$, and an R-value of $R_D = R_{film} + 3 = 3.16 \text{ m}^2 \text{ K W}^{-1}$.

Each of these heat transfer paths and their corresponding areas are presented in Figure 6.

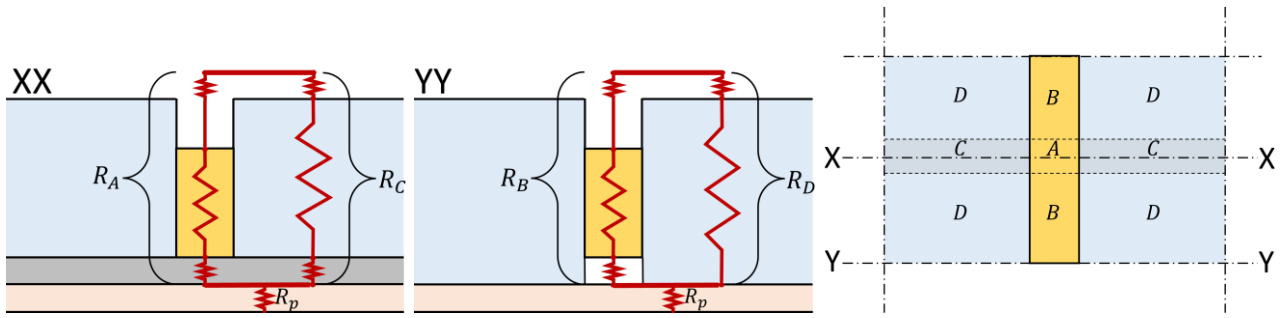


Figure 6 Example ceiling assembly showing two vertical cross-sections and a plan view indicating the heat flow paths and the areas through which they flow. Note that the batten has been made visible in the plan view diagram using dashed lines.

The correction factor F can then be calculated using Equation 2 and using the ‘steel only’ coefficients from Table 3, as follows.

$$F = 0.72 + 0.058 \left(\frac{3.16 \times 0.04}{0.6493 \times 0.09} \right) + 0.46 \left(\frac{0.9 - 0.28}{0.9} \right) - 0.29 \ln \left(\frac{0.09 + 0.02}{0.144 + 0} \right) + 0.87 \left(\frac{0.04 - 0.04}{0.04} \right)$$

$$F = 1.2405$$

Insertion of this correction factor into the modified NZS 4214 equation for the ceiling R-value (Equation 1), yields:

$$R = \sum_i R_{h_i} + \left(\frac{1}{F} \sum_j \frac{f_{tb_j}}{R_{tb_j}} + \sum_k \frac{f_{in_k}}{R_{in_k}} \right)^{-1} - R_{film}$$

$$R = R_p + \left(\frac{1}{F} \left(\frac{f_A}{R_A} + \frac{f_B}{R_B} \right) + \left(\frac{f_C}{R_C} + \frac{f_D}{R_D} \right) \right)^{-1} - R_{film}$$

$$R = 2.549 \text{ m}^2 \text{ K W}^{-1}$$

Note that the correction factor F is only applied to paths that contain the thermal bridge, and that the film resistance R_{film} is subtracted from the total R-value to arrive at a result that does not include film resistances (i.e. a ‘surface to surface’ R-value).

3.3 PERFORMANCE OF THE NEW METHOD

The following sections present an assessment of the accuracy of the new calculation method using CFD results from this study, and from our three previous studies on the same topic [5–7]. In general, we have used the root mean square (RMS) deviation between calculated R-values and those determined through CFD as the primary performance metric.

3.3.1 Performance within the Present Dataset

Figure 7 provides a comparison of R-values determined using the standard NZS 4214 method and the new method, for the 840 cases simulated in this Stage 2 of the project. Key findings include the following.

- a) Significant inaccuracies are evident in standard NZS 4214 calculations when applied to steel-framed assemblies with no thermal bridge mitigation or battens (both of which provide something of a thermal break, reducing the severity of thermal bridging).
- b) Standard NZS 4214 calculations tend to be relatively accurate for timber-framed assemblies, but inaccurate for cases where the insulation is significantly taller than the frame members and/or the frame members are encapsulated to a significant degree.
- c) These observations are consistent with the findings of our previous studies [5–7].

The new calculation method corrects for the inaccuracies above to a significant degree, reducing the RMS deviation between calculations and CFD in steel-framed cases without mitigation or battens by 87 %, i.e. from $1.289 \text{ m}^2 \text{ K W}^{-1}$ using NZS 4214 to $0.179 \text{ m}^2 \text{ K W}^{-1}$ when the new method is applied.

However, some individual cases still deviate from the benchmark CFD results by a significant margin, with a maximum difference of $0.737 \text{ m}^2 \text{ K W}^{-1}$, which equalled 22 % of the total assembly R-value in that case. Such outlying results demonstrate the limitations of the new calculation method. While

it is a significant improvement on the current NZS 4214 method for the types of ceilings and floors investigated here, it does not provide exact results in all cases.

The new method also provides a significant, although less pronounced, improvement over the NZS 4214 method for assemblies with battens, with a reduction in RMS deviation of 46 % from 0.266 to 0.144 m² K W⁻¹, and cases with thermal bridge mitigation, with a reduction in RMS deviation of 25 % from 0.158 to 0.119 m² K W⁻¹. The new method displayed similar performance in the small number of cases involving alternative boundary conditions or alternative frame spacings.

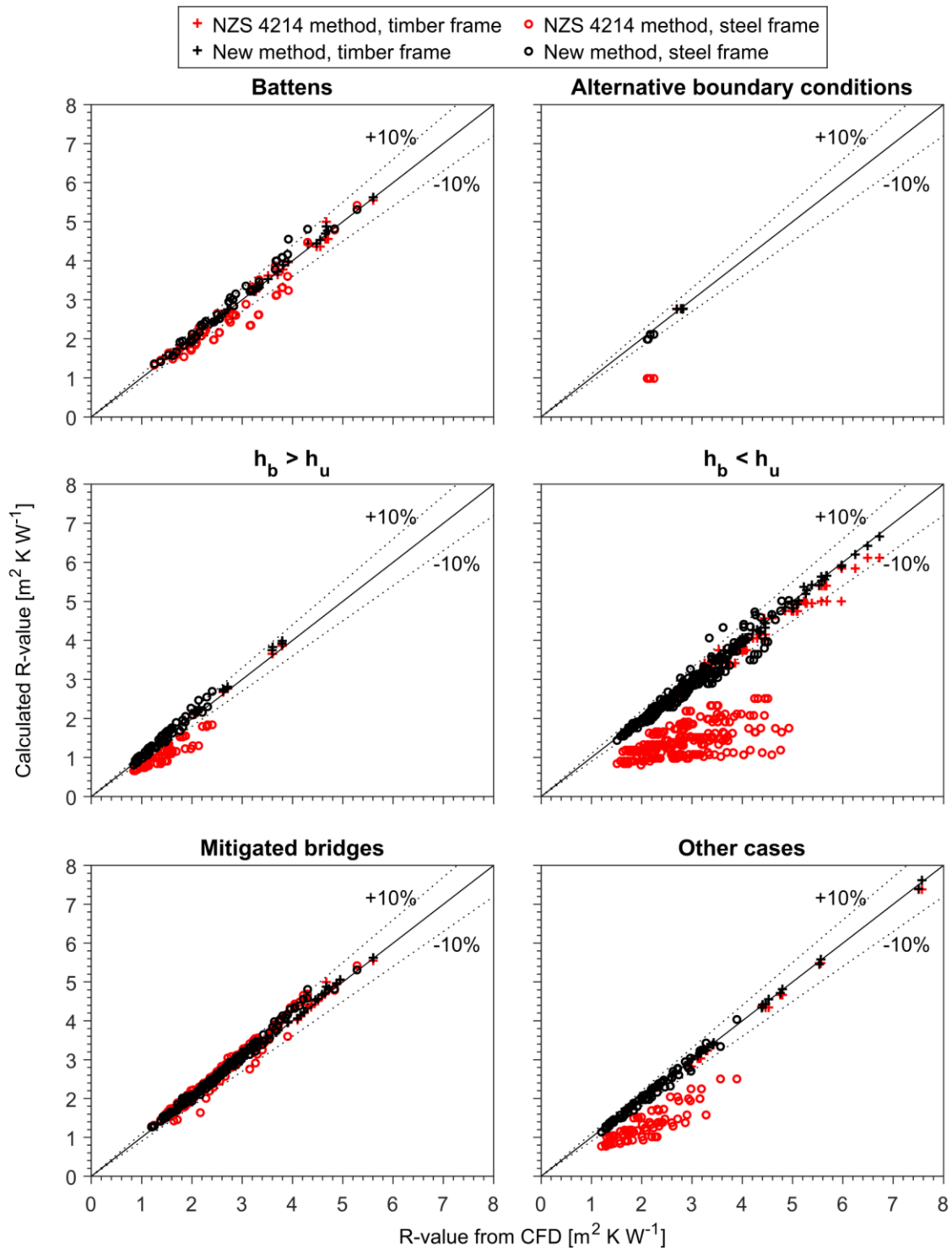


Figure 7: R-values calculated using the standard NZS 4214 method or new method developed here (with separate ‘timber only’ and ‘steel only’ models), compared to values obtained through CFD simulations. Each graph contains data from an exclusive subset of the 840 simulated cases as indicated in the heading: cases with battens and no mitigation, cases with alternative boundary conditions, cases with frame members taller or shorter than the batt insulation (symbols h_b and h_u represent the heights of frame members and insulation, respectively) and no mitigation or battens, cases with thermal bridge mitigation, and all cases not presented in any of the other graphs.

3.3.2 Validation Against Previous Results

The accuracy of the new calculation method was further tested by applying it to the cases simulated in our three previous investigations on thermal bridging [5–7]. The accuracy of standard NZS 4214 calculations, and calculations following the new method, are summarised in Table 4, and presented graphically in Figure 8, Figure 9 and Figure 10.

Differences in performance between the calculation methods were similar to those observed within the set of cases simulated in this study (and described in Section 3.3.1). The NZS 4214 calculation method produced inaccurate results when applied to steel-framed ceilings or suspended floors without thermal bridge mitigation measures or battens in place, and the new calculation method reduced that inaccuracy significantly (by between 80 and 100 %). The accuracy of calculated R-values in timber-framed cases was typically also improved by the new method, especially in cases with insulation significantly taller than the frame members and/or significant encapsulation. The accuracy of R-values predicted using the new method is typically within $\pm 10\%$, but a small number of cases (less than 5 % of all cases tested) did exceed this margin.

Table 4: Root mean square (RMS) difference between R-values obtained using various calculation methods and from CFD simulations [$m^2 K W^{-1}$].

Model	Original ABCB study [5]	NASH study [6]	Ceilings simulated in Stage 1 [7]	Floors simulated in Stage 1 [7]	This study (i.e. Stage 2)
Standard NZS 4214 method	0.690	0.695	0.435	0.497	0.859
New methods developed within each previous study ¹	0.137	N/A	0.043	0.068	N/A
New method developed in this study with single ‘timber or steel’ set of coefficients	0.123	0.114	0.185	0.123	0.168
New method developed in this study with separate ‘timber only’ and ‘steel only’ sets of coefficients	0.078	0.094	0.259	0.102	0.139

¹ Note that the methods developed in previous studies were calibrated for the specific building assemblies simulated in each study, and are therefore only applicable to a relatively narrow set of building assemblies, whereas the new method developed in this study is intended as a more generally applicable calculation method.

Table 4 not only compares the standard NZS 4214 method and new method developed in this study, but also includes information on the performance of the new methods developed in each previous study for the specific set of cases investigated (i.e. the calculation methods with ‘pseudo air-space’ R-values described in our previous reports [5–7]). While the new method proposed here reduces the inaccuracy in all datasets significantly, as compared to standard NZS 4214 calculations, it is clearly not as accurate as the type of calibrated models produced specifically for the sets of ceiling and floor

constructions considered in Stage 1 of this project. The method developed here is designed to be much more broadly applicable, and some accuracy is sacrificed in the process.

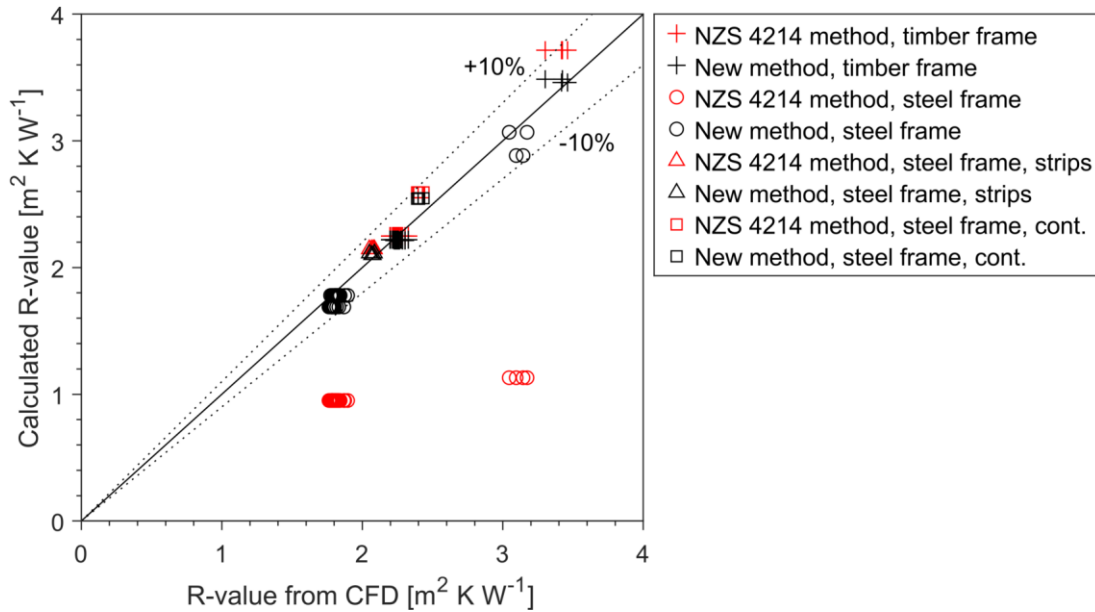


Figure 8: R-values calculated using the standard NZS 4214 method and the new method developed here (with separate ‘timber only’ and ‘steel only’ models), compared to values obtained through CFD simulations in the original thermal bridging study for the ABCB with thermal bridge mitigation options of strips or continuous layers of insulation added [5].

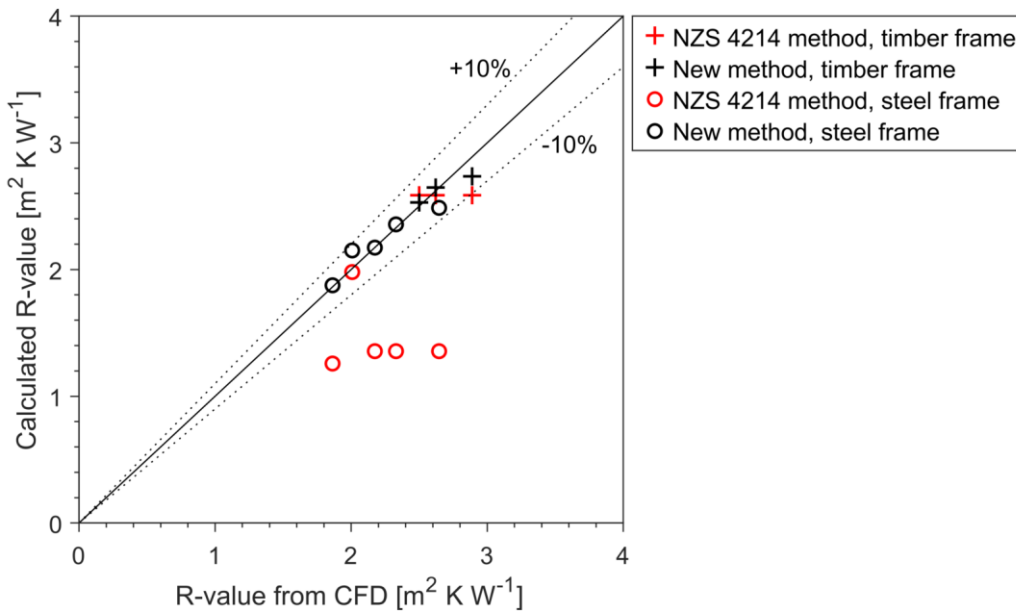


Figure 9: R-values calculated using the standard NZS 4214 method and new method developed here (with separate ‘timber only’ and ‘steel only’ models), compared to values obtained through CFD simulations in the study completed for NASH [6].

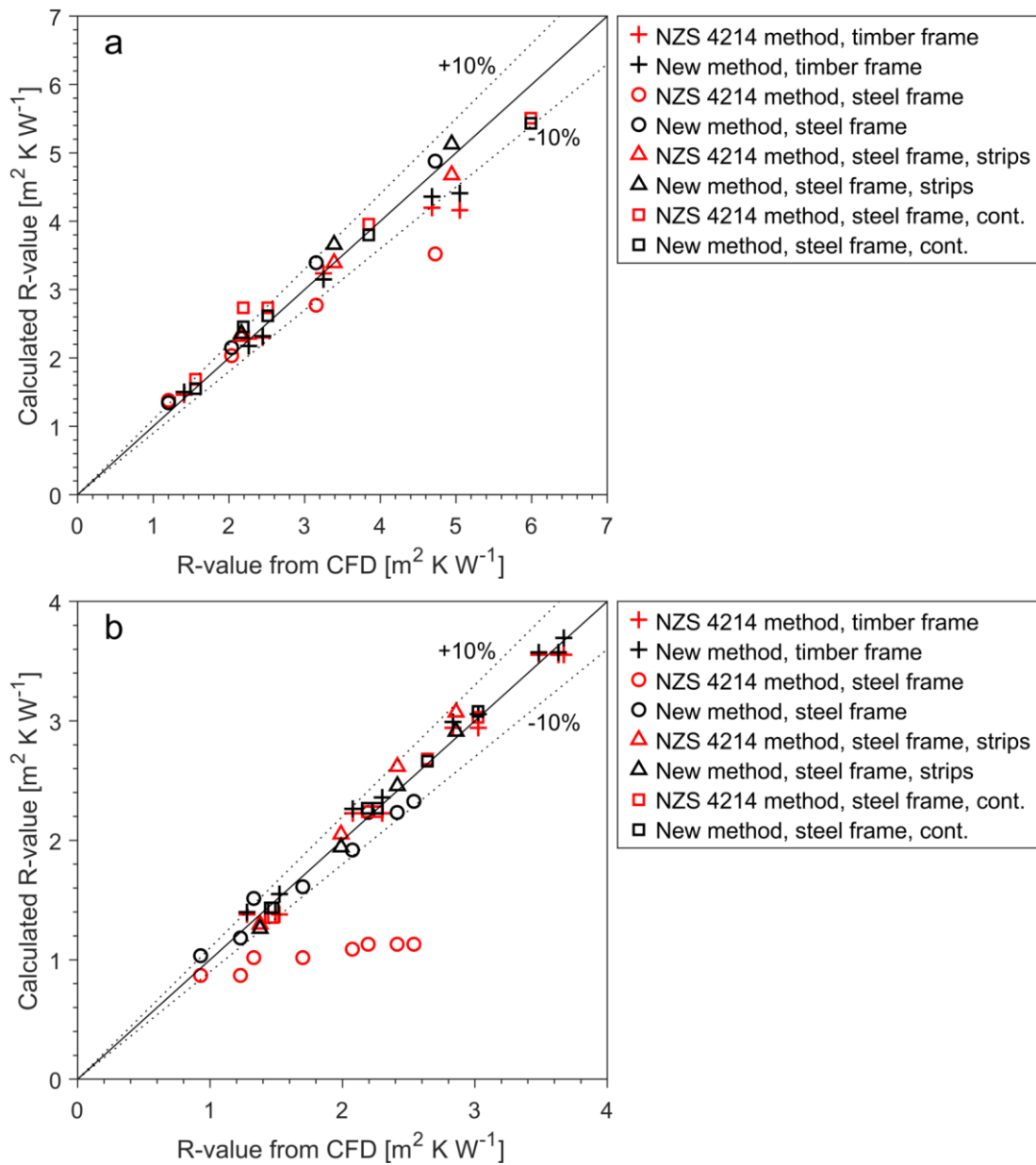


Figure 10: R-values calculated using the standard NZS 4214 method or new method developed here (with separate ‘timber only’ and ‘steel only’ models), compared to values obtained through CFD simulations in Stage 1 of this study [7], for: (a) ceilings, and (b) suspended floors.

4 Alternative DTS Mitigation Measures

In Stage 1 of the current project, an updated table of DTS thermal bridge mitigation measures was generated for steel-framed horizontal ceilings under pitched roofs [7], which was intended for possible replacement of Tables 13.2.3v and J3D7v in the draft NCC 2022. During the course of Stage 2, the ABCB requested alternative versions of the same table be generated, based on revised assumed levels of frame encapsulation, as illustrated in Figure 11.

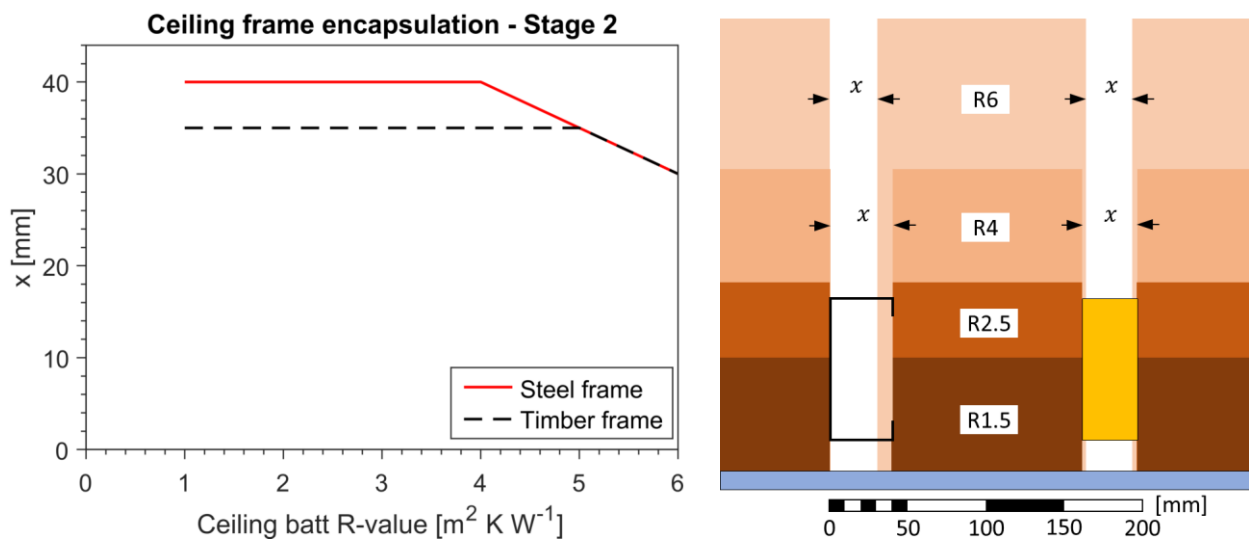


Figure 11: Alternative assumptions regarding the level of encapsulation of frame members by adjacent insulation. The dimension x represents the width of the gap between adjacent batts, above each frame member.

These requested alternative levels of encapsulation were based on two assumptions: i) the total width of batts between each pair of adjacent frame members is 40 mm narrower than the frame centre-to-centre spacing, and ii) no gaps exist between frame members and batts.

Rather than using the new method described in this report to calculate the alternative set of DTS mitigation measures, a separate set of calibrated models was developed specifically for the small subset of CFD simulations that corresponded to the cases of interest (i.e. simulations of steel-framed and timber-framed ceilings with a range of batt R-values, ceiling battens, and levels of encapsulation matching Figure 11). This approach is very similar to the approach used to generate the tables of mitigation measures in the Stage 1 report [7], and produces results that are more accurate than is possible with the more broadly applicable calculation method developed in Stage 2 (see Table 4).

These specific calibrated models took the following form:

$$F' = C'_1 + C'_2 R_{batt} \quad (3)$$

where:

F' is a correction factor that can be used in the same way as other correction factors in this report;

R_{batt} is the nominal R-value of the batts [$\text{m}^2 \text{K W}^{-1}$]; and

C'_1 and C'_2 are model coefficients.

Three sets of model coefficients were developed based on relevant CFD results, as outlined in Table 5. Within the subset of cases used to develop the models, the RMS deviation between calculated and simulated R-values was $0.069 \text{ m}^2 \text{K W}^{-1}$.

Table 5: Coefficients developed for use in Equation 3.

Ceiling configuration	Model coefficients	
	C'_1	C'_2
Timber-framed ceilings with battens and encapsulation as per Figure 11	0.814	0.0044
Steel-framed ceilings with battens and encapsulation as per Figure 11	0.597	0.100
Steel-framed ceiling with battens, encapsulation as per Figure 11 and strips of insulation installed as a thermal bridge mitigation measure	0.576	0.0396

Using these models, and the performance criteria described in the Stage 1 report [7], the alternative mitigation measures outlined in Table 6 were calculated.

A second alternative set of minimum mitigation measures were also developed, as shown in Table 7. These values are based on the timber-framed ceilings simulated in Stage 1 and the steel-framed ceilings simulated in Stage 2, and are therefore based on an assumption that timber-framed ceilings have a higher level of encapsulation than steel-framed equivalents.

As noted in our Stage 1 report, requirements to install the small quantities of additional insulation, such as those specified in Table 6 and Table 7, may not be worthwhile/practicable. For example, the highest R-value specified for continuous insulation in either table is only $0.0639 \text{ m}^2 \text{K W}^{-1}$, which is equivalent to an insulation layer approximately 1.5–3 mm thick. Therefore, alternative methods to manage thermal bridging in ceilings may be preferable.

Table 6: Alternative DTS mitigation measures for Tables 13.2.3v and J3D7v of NCC 2022. These values are based on the assumption that the total width of batts between each pair of adjacent frame members is 40 mm narrower than the frame centre-to-centre spacing.

Minimum R-value from Tables 13.2.3a to 13.2.3i, and Table 13.2.3s if applicable	Option 1 - Increase insulation between ceiling framing to specified minimum R-value	Option 2 - Add insulation strips with specified minimum R-value above or below the ceiling framing	Option 3 - Add a layer of continuous insulation with specified minimum R-value above or below the ceiling framing
1.5	1.5709	0.2510	0.0446
2.0	2.0903	0.2472	0.0473
2.5	2.5944	0.2378	0.0414
3.0	3.0788	0.2255	0.0293
3.5			
4.0			
4.5			
5.0		No mitigation required	
5.5			
6.0			

Table 7: Alternative DTS mitigation measures for Tables 13.2.3v and J3D7v of NCC 2022. These values are based on the assumption that the total width of batts between each pair of adjacent frame members is 20 mm narrower than the frame centre-to-centre spacing in timber-framed ceilings, and 40 mm narrower than the frame centre-to-centre spacing in steel-framed ceilings.

Minimum R-value from Tables 13.2.3a to 13.2.3i, and Table 13.2.3s if applicable	Option 1 - Increase insulation between ceiling framing to specified minimum R-value	Option 2 - Add insulation strips with specified minimum R-value above or below the ceiling framing	Option 3 - Add a layer of continuous insulation with specified minimum R-value above or below the ceiling framing
1.5	1.5882	0.2975	0.0555
2.0	2.1036	0.2689	0.0543
2.5	2.6297	0.2773	0.0572
3.0	3.1689	0.3019	0.0639
3.5		No mitigation required	
4.0	4.0112	0.2110	0.0031
4.5	4.5501	0.2458	0.0125
5.0	5.0979	0.2800	0.0221
5.5	5.6535	0.3133	0.0317
6.0	6.2158	0.3457	0.0411

5 Conclusion

The new calculation method developed in this study provides an improved means to estimate the R-value of a broad set of ceiling or suspended floor assemblies.

It is significantly more accurate than the standard NZS 4214 method when applied to: i) assemblies with steel thermal bridges that are not mitigated by additional insulation or thermally broken by battens, and ii) timber-framed assemblies in which the frame members are significantly shorter than the surrounding bulk insulation. The RMS inaccuracy in these categories of cases was reduced by 87 % and 89 %, respectively, when the new method was adopted rather than the standard NZS 4214 method.

In other cases (e.g. those with battens or thermal bridge mitigation measures in place), the new method typically provides some improvement in accuracy, but the benefits are less consistent.

We recommend that the new method be used when calculating the R-value of ceiling or floor assemblies that include a thermally bridged layer directly exposed to the adjacent air space, rather than using standard methods such as those contained in NZS 4214 and ISO 6946, the Modified Zone method, and the Gorgolewski method.

While the overall improvements in accuracy across a broad range of construction configurations is significant, one should keep in mind that the new calculation method is not as reliable as thermal bridge performance data from experiments or numerical simulations (e.g. CFD). For applications that require a higher level of accuracy than the $\pm 10\%$ (with 95 % confidence) achieved by the new method presented here, we recommend that CFD simulations or experiments be conducted for the specific cases of interest. Empirical corrections to one-dimensional hand calculation methods (such as NZS 4214) can then be developed that are accurate for the very narrow range of construction types that are of interest (e.g. the sets of ceiling and suspended floor assemblies covered in Stage 1 of this project).

The value of the new calculation method therefore lies in its broad applicability. It has been developed and validated for a wide variety of construction details, and addresses the primary sources of inaccuracy that affect the NZS 4214 method when it is applied to ceilings or suspended floors. For general use in estimating the R-values of such building assemblies, where the thermally bridged layer is exposed directly to an adjacent air space, the new calculation method presented here is significantly more reliable than other existing thermal bridge calculation methods.

References

- [1] Standards New Zealand, NZS 4214:2006 Methods of Determining the Total Thermal Resistance of Parts of Buildings, (2006).
- [2] International Organization for Standardization, ISO 6946 Building components and building elements - Thermal resistance and thermal transmittance - Calculation methods, (2017).
- [3] J. Kosny, J.E. Christian, Reducing the uncertainties associated with using the ASHRAE zone method for R-value calculations of metal frame walls, in: American Society of Heating, Refrigerating and Air-Conditioning Engineers, Inc., Atlanta, GA (United States), United States, 1995. <https://www.osti.gov/biblio/211841>.
- [4] M. Gorgolewski, Developing a simplified method of calculating U-values in light steel framing, Building and Environment. 42 (2007) 230–236. <https://doi.org/https://doi.org/10.1016/j.buildenv.2006.07.001>.
- [5] A. Green, L. Kempton, P. Cooper, G. Kokogiannakis, Thermal Bridging of Horizontal Ceilings under Pitched Roofs, 2021.
- [6] A. Green, S. Beltrame, P. Cooper, Thermal bridging by ceiling frame members, 2021.
- [7] A. Green, S. Beltrame, G. Kokogiannakis, P. Cooper, Repeating Thermal Bridges in Ceilings and Floors: Simulation and Calculation, Wollongong, Australia, 2022.
- [8] ASHRAE, 2017 ASHRAE Handbook Fundamentals, The American Society of Heating, Refrigerating and Air-Conditioning Engineers, Atlanta, GA, USA, 2017.
- [9] S.M. Doran, M.T. Gorgolewski, BRE Digest 465: U-values for light steel-frame construction, Building Research Establishment, Watford, UK, 2002.
- [10] H.A. Trethowen, Validating the Isothermal Planes Method for R-Value Predictions, ASHRAE Transactions. 101 (1995) 755–766.

Appendices

APPENDIX A: CFD METHODOLOGY

The CFD simulations described in this report were based on a finite-volume formulation of the Reynolds-averaged Navier Stokes (RANS) equations. The shear stress transport (SST) $k-\omega$ turbulence model was used, with low-Reynolds number treatment near walls (the mesh was kept fine enough near walls to maintain a dimensionless near-wall distance, y^+ , less than one). In cases involving small, restricted air spaces, laminar flow was simulated in those small air spaces.

Buoyancy effects were simulated using the Boussinesq approximation. Radiant heat transfer between surfaces bounding the roof space was simulated using the discrete ordinates model, and by treating all surfaces as opaque, grey and diffuse.

The simulations were run using the coupled pressure-based solver in ANSYS Fluent, and adopting the PRESTO! scheme for spatial discretisation of pressure and second-order upwind discretisation for all other field variables.